Monte Carlo simulations of diluted magnetic semiconductors using *ab initio* exchange parameters

2009 J. Phys.: Condens. Matter 21 064238

(http://iopscience.iop.org/0953-8984/21/6/064238)

J. Phys.: Condens. Matter **21** (2009) 064238 (6pp) doi:10.1088/0953-8984/21/6/064238

Monte Carlo simulations of diluted magnetic semiconductors using *ab initio* exchange parameters

S K Nayak[1], M Ogura[2], A Hucht[1], H Akai[2] and P Entel[1]

[1] Physics Department, University of Duisburg-Essen, 47048 Duisburg, Germany
[2] Department of Physics, Osaka University, 1-1 Machikaneyama, Toyonaka, Osaka 560-0043, Japan

E-mail: sanjeev.nayak@uni-due.de

Received 18 July 2008, in final form 30 October 2008
Published 20 January 2009
Online at stacks.iop.org/JPhysCM/21/064238

Abstract

Co doped ZnO ($Zn_{1-x}Co_xO$) is studied as a prototype material for transition metal doped II–VI diluted magnetic semiconductors (DMSs) from first-principles and Monte Carlo simulations. The exchange interactions are calculated using the Korringa–Kohn–Rostoker (KKR) Green's function method. The exchange coupling constants thus obtained are treated in the classical Heisenberg model and the magnetic phase transitions are studied by the Monte Carlo technique. Our results show that the defect free substitutional DMSs of $Zn_{1-x}Co_xO$ do not sustain magnetization at low concentration. At high concentration, we find layered magnetic structures. Ferromagnetism, with Curie temperature below room temperature, is stable at intermediate Co concentrations. First-principles studies with the generalized gradient approximation (GGA) and the GGA together with the Hubbard U are discussed with respect to structural and electronic properties of ZnO.

(Some figures in this article are in colour only in the electronic version)

1. Introduction

It is desirable to have a class of materials possessing semiconducting and magnetic properties to help make devices for a variety of applications, for example, semiconducting devices having spin dependent transport properties. Diluted magnetic semiconductors (DMSs), where semiconductors are doped with a very dilute concentration of magnetic ions, are believed to suffice for the purpose. While various types of magnetism can be encountered in such materials, occurrence of room temperature ferromagnetism is of primary interest for practical applications, so that both the spin and the charge degree of freedom can play a decisive role. Reviews of DMSs can be found in [1–3]. Up till now the fundamental understanding of magnetism in this class of materials is system specific and not general. For example, magnetism in Mn doped GaAs is believed to be carrier mediated, which is attributed to the presence of an extra hole per dopant in the system. Based on studies from the effective Ginzburg–Landau free-energy approach, Dietl *et al* have shown that, out of several semiconductors, GaN and ZnO could attain room temperature ferromagnetism under specific conditions [4]. These binary semiconductors are the focus of thorough studies both experimentally and theoretically. ZnO in particular is a prospective material in bulk and nanoparticles because of its strong light-emitting properties [5], and when doped suitably forms highly transparent conducting oxides for sensor and solar cell applications. Recently, there has been much discussion on ferromagnetism observed in DMSs based on ZnO. While some experiments show ferromagnetism [6–12], others suggest a spin-glass state of magnetic ordering resulting in no significant magnetization in the system [13, 14]. A similar unclear situation also prevails in the theoretical studies [15–23].

In this work, we studied the electronic structure of pure ZnO and magnetism in Co doped ZnO by the *ab initio* density functional approach and Monte Carlo simulations using a classical spin model. In particular, we highlight in this paper the change of magnetic order from ferromagnetism for $x \geqslant 0.2$ to antiferromagnetism with alternating ferromagnetic bi-layers

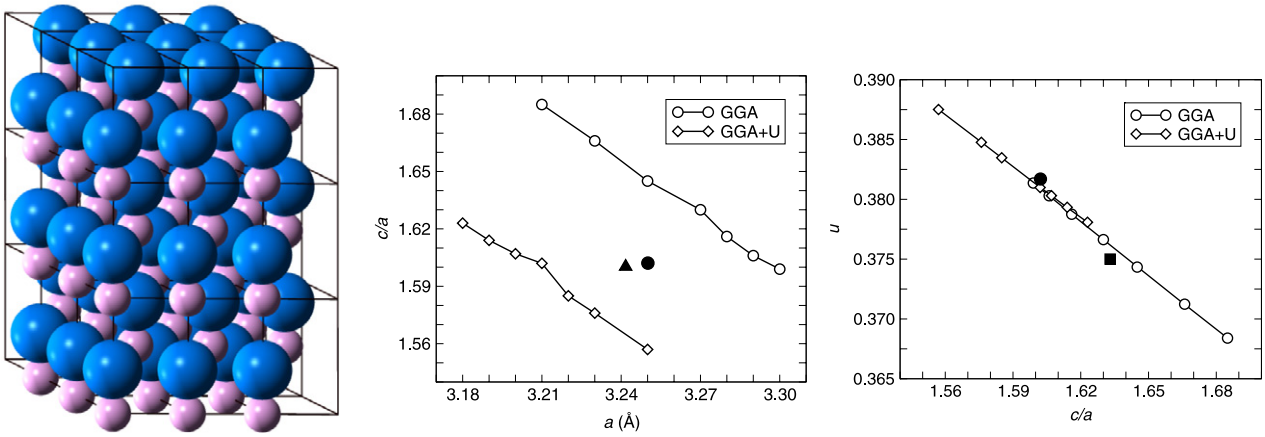

Figure 1. (a) A supercell of wurtzite lattice consisting of 3 × 3 × 3 unit cell repetitions. The light and dark colors represent Zn and O atoms, respectively, The radii of spheres are scaled to schematically represent Zn^{2+} and O^{2-}. (b) Comparison of minimum energy lattice parameters a and c/a of ZnO for GGA and GGA + U (U_{eff} on the Zn d orbital is 7.5 eV, see the text). The experimental values are given by the filled circle [34] and filled up-triangle [35]. (c) The variations of u and c/a obtained by relaxing the lattice for various c/a values are compared for GGA and GGA + U. The filled circle shows the experimental value [34], while the filled square shows the perfect value of $u = 0.375$ and $c/a = 1.633$.

for $x \geqslant 0.75$ in $Zn_{1-x}Co_xO$. Part of the work with respect to the present paper is published elsewhere [24].

2. Computational method

ZnO was studied by density functional theory (DFT) in combination with the generalized gradient approximation (GGA) as the description of the exchange and correlation functional as proposed by Perdew and Wang [25]. The atomic valency states for Zn, O and Co were $3d^{10}4s^2$, $2s^22p^4$ and $3d^74s^2$, respectively, which were treated by pseudopotentials together with the projector augmented wave method (PAW) [26] implemented in the Vienna *Ab Initio* Simulation Package (VASP) [27, 28]. The electronic wavefunctions were expanded in a plane-wave basis set with an energy cutoff of 400 eV. The Brillouin zone integration was performed with weighted points selected by the Monkhorst–Pack algorithm from an 11 × 11 × 11 k-space grid. We have adopted the formulation proposed by Dudarev *et al* [29] for GGA + U calculations. According to this, the total energy is a function of U_{eff} given by the relation

$$E_{\text{GGA}+U} = E_{\text{GGA}} + \frac{U_{\text{eff}}}{2}\sum_{m\sigma}(n_{m\sigma} - n_{m\sigma}^2), \qquad (1)$$

where $U_{\text{eff}} = U - J$, with U and J representing the spherically averaged on-site Coulomb interaction and screened exchange integrals, respectively; $n_{m\sigma}$ is the occupancy of the orbital with magnetic quantum number m and spin σ. For a comprehensive discussion we refer to the literature [29, 30]. The value of J was kept fixed at $J = 1$ eV for d orbitals in our calculations, thus $U = 1$ eV corresponds to the pure GGA limit, since in this case $U_{\text{eff}} = 0$ eV. We have $U_{\text{eff}} = 7.5$ eV for Zn d orbitals to be consistent with previous studies [31].

The effective coupling constants, J_{ij}, were calculated using the first-principles Korringa–Kohn–Rostoker (KKR) Green's function method with the coherent potential approximation (CPA) together with the local density approximation (LDA) according to the formulation proposed by Liechtenstein *et al* [32]. The calculations were done using the Machikaneyama-2002 code [33]. The J_{ij} thus obtained are used as input for Monte Carlo simulations of a classical Heisenberg model with $|\mathbf{S}| = 1$ and Hamiltonian

$$H_{\text{cl}} = -\tfrac{1}{2}\sum_{ij} J_{ij}\mathbf{S}_i \cdot \mathbf{S}_j. \qquad (2)$$

3. Results and discussion

3.1. Crystal structure and electronic structure of ZnO in DFT

We have used the wurtzite crystal lattice (figure 1(a)) for studying ZnO. We began by looking at the minimum energy lattice parameters in GGA and GGA + U, where, for each a, energies of various c/a ratios were calculated. The lattice was relaxed to minimize local strain, and thus a suitable u parameter is approached at each step. The variation of a versus c/a for GGA and GGA+U is shown in figure 1(b). Figure 1(c) shows the value of u obtained corresponding to the c/a found for each a. The minimum energy structural parameters of ZnO for GGA and GGA + U are found to be $a = 3.290$ Å, $c/a = 1.606$, $u = 0.380$, and $a = 3.190$ Å, $c/a = 1.614$, $u = 0.379$, respectively. We find a slightly higher value of a, and as a result slightly lower values of c/a and u, in comparison to Erhart *et al* [31]. The experimental value of a lies in between the GGA and GGA + U values, shown as the filled up-triangle [34] and filled circle [35] in figure 1(b). The values of c/a and u are close to the GGA values. Variations of u and c/a match for GGA and GGA + U as shown in figure 1(c). It is well known that the electronic structure of ZnO described by GGA (in fact for all semiconductors) gives a lower bandgap than the experimental values.

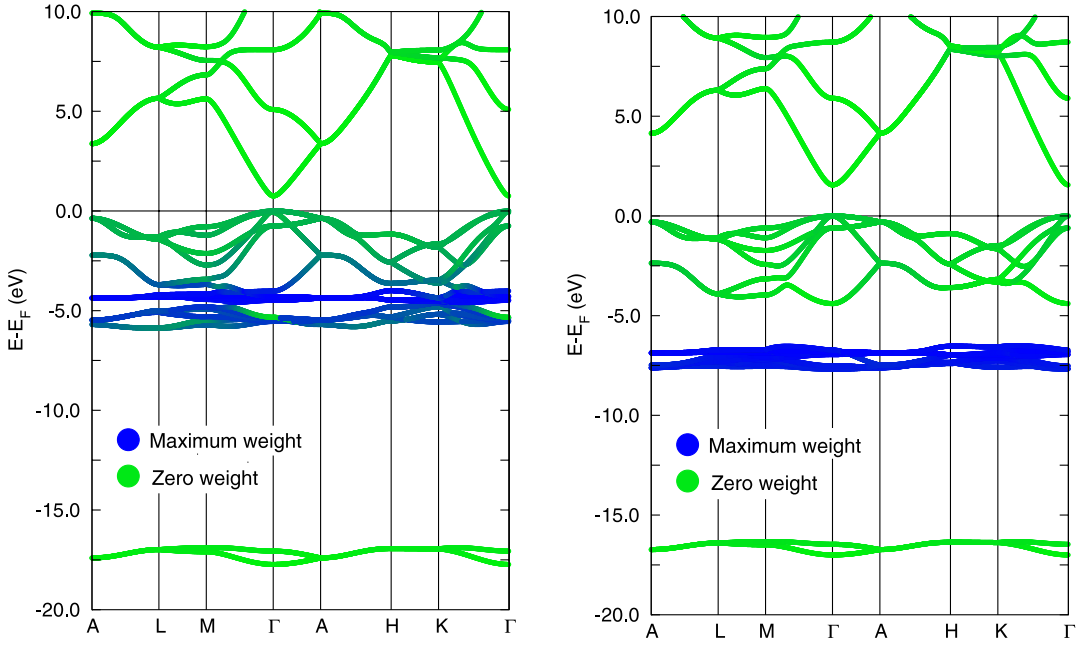

Figure 2. Zn 3d contribution to the band structure of ZnO according to maximum and zero weight in GGA (left) and GGA + U (right). Left: one observes that the bandgap is low compared to experimentally accepted values of 3.44 eV. The hybridization of Zn 3d orbitals and the O 2p is overestimated. Right: by introducing the Hubbard U, where U_{eff} for Zn 3d is 7.5 eV, we get an improvement in the hybridization of Zn 3d and O 2p.

The difference in bandgap compared to experiments is greater for ionic solids compared to covalent ones. The Bader charge analysis [36] gives an ionic nature of $Zn^{+(2-\delta)}O^{-(2-\delta)}$, where $\delta = 0.75$. GGA also fails to describe the energy location of Zn d bands with respect to the Fermi energy (here valence band maxima) in ZnO. The action of the Hubbard term is to shift the unoccupied states to higher energy by $U/2$ and the occupied states to lower energy by the same value. The energy difference between GGA and GGA + U as given by equation (1) is non-zero only for partially filled orbitals. For completely filled or completely empty orbitals it is zero since $n = n^2$ for $n = 1$ or 0. Therefore, using a finite n value for the more or less completely occupied d levels of the Zn atoms must be considered with caution. In figure 2, GGA (left) and GGA + U (right) band structures of ZnO are compared. By adding extra on-site correlation on orbitals like Zn d, Zn s and O p orbitals, we find a linear increase in E_g with increasing U, but with different slopes [24]. With $U_{\text{eff}} = 7.5$ eV for Zn d orbitals, the value of the bandgap is 1.57 eV, which is still 50% of the experimentally accepted value of 3.44 eV; GGA however gives $E_g = 0.69$ eV. The energy location of Zn d bands now matches the experimental value [38]. The Zn d bands are more localized in GGA+U. Thus the hybridization between Zn 3d and O 2p orbitals is improved, which was overestimated in GGA. This is in accordance with the ionic bonding description of ZnO, where only Zn s and O p orbitals participate in bonding.

Orbital decomposition of the ZnO band structure shows that the conduction band minimum consists of only s character contributed from Zn, hence the increase of bandgap is not as monotonic as the energy shift of d bands with increasing U_{eff} on Zn d orbitals. Considering the effective U for the Zn s together with the Zn d orbitals might help to achieve the experimental bandgap. A similar approach is adopted by Walsh *et al* [37] to describe the electronic states in their argument favoring carrier mediated ferromagnetism in $Zn_{1-x}Co_xO$.

Several authors have adopted self-interaction corrected (SIC) DFT instead of Hubbard U [22, 39–44] to describe the electronic properties of this material. With SIC, one gets a shift of Zn d orbital to lower energies and the bandgap improves reasonably well. However, some properties like structural phase transitions are inappropriately described [45].

We discuss the effect of GGA + U on the electronic structure of $Zn_{1-x}Co_xO$ for the sake of completeness. Incorporating U_{eff} in Zn and Co d orbitals shifts both the Zn d states and Co d states to lower energies. The density of states obtained for $Zn_{0.875}Co_{0.125}O$, with $U_{\text{eff}} = 7.5$ eV and 5.0 eV for Zn 3d and Co 3d, respectively, is shown in figure 3. The density of states is in agreement with the SIC calculations [39, 40] and matches the experimentally observed photoemission measurements [46], peak positions of which are shown by arrows. The DOS is also in agreement with the photoemission measurements by Wi *et al* [47], where they show that the Co 3d states lie at the top of the O 2p band. They do not observe any long range ferromagnetic behavior in their samples.

3.2. Exchange interactions in $Zn_{1-x}Co_xO$

The experimental lattice constants chosen for the calculations of J_{ij} for all compositions in steps of 1% up to $x = 0.1$ and then in intervals of 10% up to $x = 1.0$. Figure 4(a) shows the variation of J_{ij} with Co concentration for several neighboring distances between Zn sites. Dramatic changes in J_{ij} for the

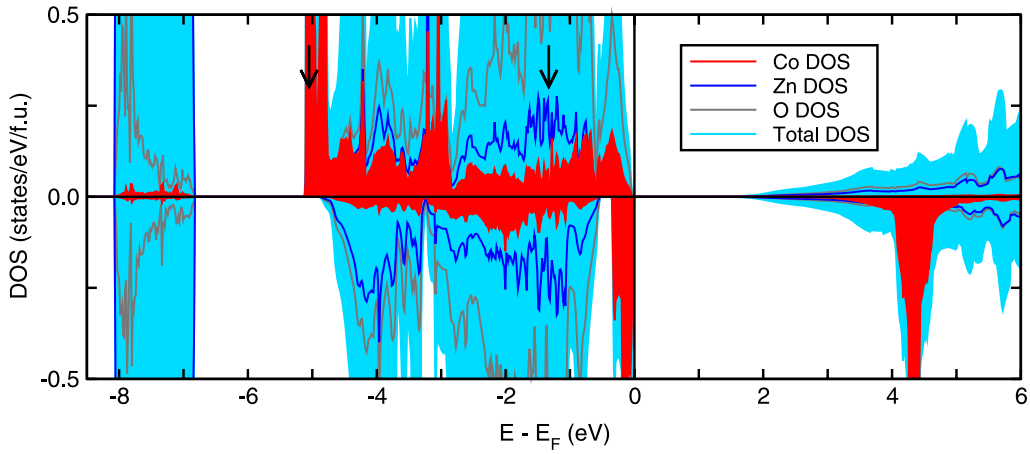

Figure 3. Density of states (DOS) of $Zn_{0.875}Co_{0.125}O$ in GGA + U with U_{eff} for 3d orbitals of Zn and Co as 7.5 and 5.0 eV, respectively. This plot is comparable to SIC calculations [39, 40]. The arrows show the peak positions found in the photoemission experiments [46].

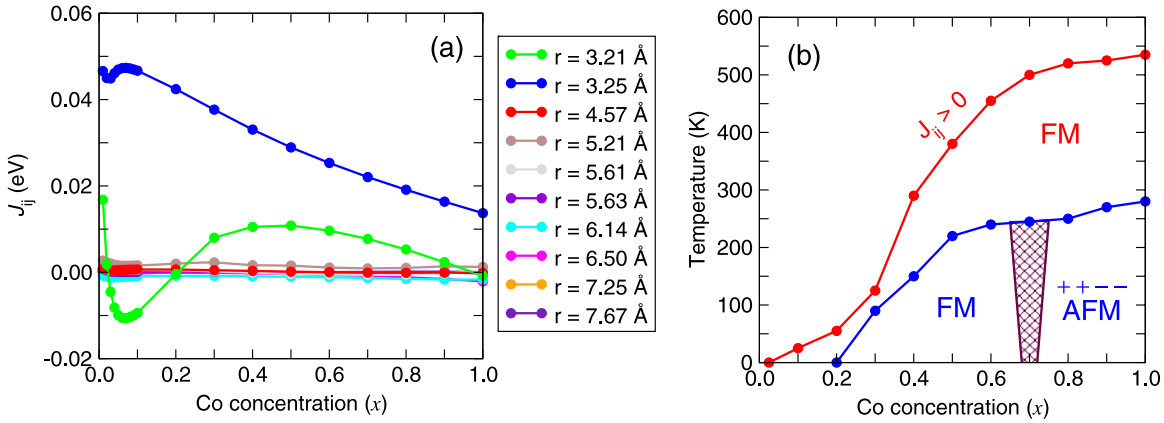

Figure 4. The left panel shows the concentration dependent exchange coupling J_{ij} for various neighboring distances r between Zn sites in $Zn_{1-x}Co_xO$. (b) The right panel shows the magnetic phase diagram of $Zn_{1-x}Co_xO$. The system sustains ferromagnetism with low Curie temperature for $0.2 \leqslant x \leqslant 0.65$. Antiferromagnetic alignment with alternating ferromagnetic layers, represented by $++--$, is stable for large concentrations. The red curve shows the phase boundary calculated with all couplings positive, $J'_{ij} = |J_{ij}|$.

nearest neighbor is observed with composition, which goes from positive (ferromagnetic) to negative (antiferromagnetic) and back to positive, within a concentration range of $x > 0$ to $x \approx 0.2$. For very high concentrations ($x \approx 1.0$), however, it is again antiferromagnetic. The contribution of the next nearest neighbor J_{ij} is positive, and reduces smoothly with Co concentration, except for a kink at the very low concentration. The magnitude of J_{ij} at larger distances is comparably small and flat as a function of Co concentration. The J_{ij} are oscillatory in real space as a function of distance.

3.3. Monte Carlo simulations

Co atoms are randomly distributed in the ZnO for every composition studied by Monte Carlo simulation. The phase diagram in figure 4(b) ought to be compared with J_{ij} for various compositions shown in figure 4(a), the discussion of which can be made in four parts.

3.3.1. Region I, $0 \leqslant x \leqslant 0.2$. Within this composition range, the J_{ij} for larger distances are probabilistically more important. It is observed from figure 4(a) that the J_{ij} are flat and oscillating in real space for large distances. This suggests that the system is magnetically frustrated and thus unable to keep long range order. This is clearly observed in the simulation results (blue curve in figure 4(b)). The red curve in figure 4(b) is a reference curve simulated by taking $J'_{ij} = |J_{ij}|$. In the reference curve ferromagnetism develops from $x = 0.025$. Thus, no net magnetization in this composition range is explained to be a consequence of the oscillatory nature of J_{ij}.

Taking the exchange interactions for the first and second nearest neighbor distances and using the mean-field expression of equation (3), we get the Curie temperature of 43 K for $Zn_{0.95}Co_{0.05}O$ using

$$k_B T_x^{\text{MFA}} = \tfrac{1}{3} x M^2 \sum_{j(\neq i)} J_{ij}, \tag{3}$$

where x is the concentration of Co in ZnO and k_B is the Boltzmann's constant. One must note that the role of nearest and next nearest neighbor interactions are negligible when

the concentration range in discussion is below the percolation limit. In most cases the Monte Carlo transition temperatures are lower than the mean-field predictions [24].

3.3.2. Region II, $0.2 \leqslant x \leqslant 0.65$. Concentrations in the $0.2 \leqslant x \leqslant 0.65$ range stabilize ferromagnetism. The Curie temperature is observed to rise with increase in Co concentration. As seen from figure 4(a), the magnetic interactions for both nearest and next nearest neighbors are ferromagnetic and they possess significant interaction strength. So, with respect to the overall negative J_{ij} contribution, the positive contribution wins, which leads to ferromagnetic phase.

3.3.3. Region III, $0.65 \leqslant x \leqslant 1.0$. At $x > 0.65$, the system develops magnetic configurations where ferromagnetism is observed in layers along the hexagonal plane. This is shown in the layered magnetization versus temperature plot in figure 5. From figure 4(a) we observe that the nearest neighbor J_{ij} (nn distance along the *c*-axis) is small in comparison with the next nearest J_{ij} (nn along the hexagonal plane), which are positive and significant, hence layered ferromagnetic structures are possible in this composition range. A detailed analysis for $x > 0.65$ shows that the system acquires a complicated phase of antiferromagnetically aligned ferromagnetic layers represented by $++--$, where $+$ and $-$ is the orientation of average magnetic moment in the layers with respect to some reference layer. At $x \approx 0.65$, the system goes from ferromagnetic to layered antiferromagnetic phase, which is shown as the shaded region in the phase diagram of figure 4(b). The blue curve in figure 4(b) for $0.65 \leqslant x \leqslant 1.0$ composition essentially shows the order–disorder transition for the layered magnetic state.

3.3.4. Region IV, $x = 1.0$. This is the case of pure CoO in wurtzite structure. In nature, CoO occurs in the fcc crystal lattice structure, which is antiferromagnetic with a Neél temperature of 291 K [48]. For $x = 1$, the system still has layered $++--$ phase for a majority of Co spins. This gives rise to a complicated magnetic ground state of CoO. The transition temperature from this complicated ordered state to the disordered state is found to be 280 K. This transition temperature reasonably coincides with the experimental Neél temperature of CoO, suggesting the accuracy of J_{ij}.

The phase diagram of figure 4(b) clearly suggests that there is no net magnetization observed for composition below $x = 0.2$ in $Zn_{1-x}Co_xO$. The ferromagnetic phase which is obtained for $0.2 \leqslant x \leqslant 0.65$ composition has Curie temperature below the room temperature. In the real material, a composition range of $x > 0.2$ is already too high to achieve a homogeneous distribution of substituted Co in ZnO. This may support the presence of multiple phases as a possible explanation, which has been predicted recently [49, 50], to explain the room temperature ferromagnetism in ZnO DMSs.

4. Conclusion

ZnO and substitutional Co doped ZnO are studied by DFT and Monte Carlo methods. Some aspects of ZnO, like overestimation of Zn 3d and O 2p hybridization and underestimation of the bandgap, are discussed with respect to DFT calculations within the GGA. Improvement on some of these aspects is shown to be achieved by applying on-site Hubbard U correlations. While the hybridization picture is convincingly improved, the bandgap obtained is still below the experimental value.

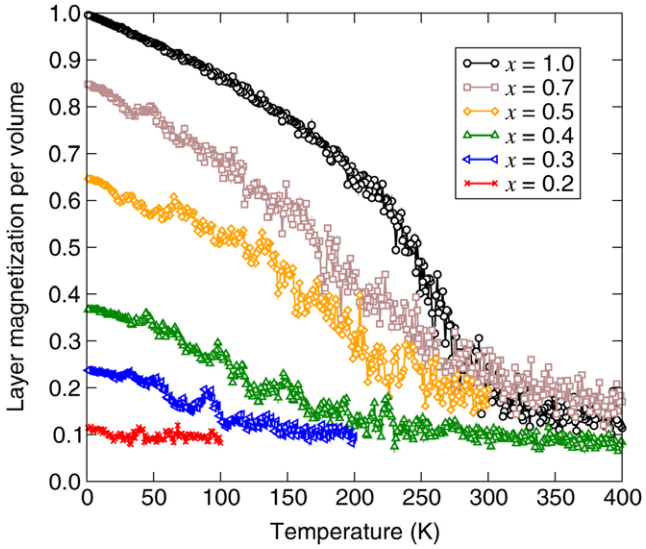

Figure 5. (a) Layer magnetization versus temperature of $Zn_{1-x}Co_xO$ for $x \geqslant 0.2$.

The distance dependent exchange coupling was calculated from KKR-CPA-LDA for the whole range of x for $Zn_{1-x}Co_xO$. The J_{ij} so obtained are used in Monte Carlo simulations for the classical Heisenberg model to study the magnetic properties of the system. We find no net spontaneous magnetization below a concentration of $x = 0.20$. The system sustains ferromagnetism for $0.20 \leqslant x \leqslant 0.65$, the Curie temperature of which is lower than room temperature. The system acquires a $++--$ type of layered magnetization for very high Co concentration. The ordered to disordered transition temperature for CoO ($x = 1.0$) is found to be close to the experimental Neél temperature of the fcc CoO antiferromagnet.

Acknowledgments

Financial support from the Deutsche Forschungsgemeinschaft through the Research Training Group GRK 1240 'Photovoltaics and optoelectronics from nanoparticles' is gratefully acknowledged. SKN would also like to thank Shreekantha Sil for fruitful discussions.

References

[1] Liu X and Furdyna J K 2006 *J. Phys.: Condens. Matter* **18** R245
[2] Janisch R, Gopal P and Spaldin N A 2005 *J. Phys.: Condens. Matter* **17** R657
[3] Prellier W, Fouchet A and Mercey B 2003 *J. Phys.: Condens. Matter* **15** R1583

[4] Dietl T, Ohno H, Matsukura F, Cibert J and Ferrand D 2000 *Science* **287** 1019
[5] Özgür Ü, Alivov Ya I, Lie C, Teke A, Reshchikov M A, Doğan S, Avrutin V, Cho S-J and Morkoç H 2005 *J. Appl. Phys.* **98** 041301
[6] Kittilstved K R, Schwartz D A, Tuan A C, Heald S M, Chambers S A and Gamelin D R 2006 *Phys. Rev. Lett.* **97** 037203
[7] Xu X, Qin X, Jiang F, Li X, Chen Y and Gehring G A 2008 *Appl. Surf. Sci.* **254** 4956
[8] Duan L B, Rao G H, Yu J and Wang Y C 2008 *Solid State Commun.* **145** 525
[9] Venkatesan M, Fitzgerald C B, Lunney J G and Coey J M D 2004 *Phys. Rev. Lett.* **93** 177206
[10] Parter J T, Ramachandran S, Tiwari A and Narayan J 2006 *J. Electron. Mater.* **35** 852
[11] Bhatti K P, Malik V K and Chaudhary S 2008 *J. Mater. Sci. Mater. Electron.* **19** 849
[12] Akdogan N, Nefedov A, Westerholt K, Zabel H, Becker H-W, Somsen C, Khaibullin R and Tagirov L 2008 *J. Phys. D: Appl. Phys.* **41** 165001
[13] Ney A, Ollefs K, Ye S, Kammermeier T, Ney V, Kaspar T C, Chambers S A, Wilhelm F and Rogalev A 2008 *Phys. Rev. Lett.* **100** 157201
[14] Kaspar T C, Droubay T, Heald S M, Nachimuthu P, Wang C, Shutthanandan V, Johnson C A, Gamelin D R and Chambers S A 2008 *New J. Phys.* **10** 055010
[15] Dietl T, Ohno H and Matsukura F 2001 *Phys. Rev.* B **63** 195205
[16] Sato K and Katayama-Yoshida H 2000 *Japan. J. Appl. Phys.* **39** L555
[17] Dietl T 2002 *Semicond. Sci. Technol.* **17** 377
[18] Sato K, Dederichs P H and Katayama-Yoshida H 2003 *Europhys. Lett.* **61** 403
[19] Sato K, Dederichs P H, Katayama-Yoshida H and Kudrnovský J 2004 *J. Phys.: Condens. Matter* **16** S5491
[20] Coey J M D, Venkatesan M and Fitzgerald C B 2005 *Nat. Mater.* **4** 173
[21] Dederichs P H, Sato K and Katayama-Yoshida H 2005 *Phase Transit.* **78** 851
[22] Gopal P and Spaldin N A 2006 *Phys. Rev.* B **74** 094418
[23] Chanier T, Sargolzaei M, Opahle I, Hayn R and Koepernik K 2006 *Phys. Rev.* B **73** 134418
[24] Nayak S K, Ogura M, Hucht A, Buschmann S, Akai H and Entel P 2008 *Phys. Status Solidi* a **205** 1839
[25] Perdew J P and Wang Y 1992 *Phys. Rev.* B **45** 13244
[26] Blöchel P E 1994 *Phys. Rev.* B **50** 17953
[27] Kresse G and Furthmüller J 1996 *Phys. Rev.* B **54** 11169
[28] Kresse G and Joubert D 1999 *Phys. Rev.* B **59** 1758
[29] Dudarev S L, Botton G A, Savrasov S Y, Humphreys C J and Sutton A P 1998 *Phys. Rev.* B **57** 1505
[30] Anisimov V I, Zaanen J and Andersen O K 1991 *Phys. Rev.* B **44** 943
[31] Erhart P, Albe K and Klein A 2006 *Phys. Rev.* B **73** 205203
[32] Liechtenstein A I, Katsnelson M I, Antropov V P and Gubanov V A 1987 *J. Magn. Magn. Mater.* **67** 65
[33] Akai H 1998 *Phys. Rev. Lett.* **81** 3002
[34] Kisi E H and Elcombe M M 1989 *Acta Crystallogr.* C **45** 1867
[35] Albertsson J, Abrahams S C and Kvick Å 1989 *Acta Crystallogr.* B **45** 34
[36] Bader R F W 1990 *Atoms in Molecules—a Quantum Theory* (New York: Oxford University Press)
[37] Walsh A, Da Silva J L F and Wei S-H 2008 *Phys. Rev. Lett.* **100** 256401
[38] Powell R A, Spicer W E and McMenamin J C 1971 *Phys. Rev. Lett.* **27** 97
[39] Katayama-Yoshida H, Sato K, Fukushima T, Toyoda M, Kizaki H and Dinh V A 2008 *J. Korean Phys. Soc.* **53** 1
[40] Toyoda M, Akai H, Sato K and Katayama-Yoshida H 2006 *Physica* B **376/377** 647
[41] Pollmann J, Krüger P, Rohlfing M, Sabisch M and Vogel D 1996 *Appl. Surf. Sci.* **104/105** 1
[42] Vogel D, Krüger P and Pollmann J 1995 *Phys. Rev.* B **52** R14316
[43] Zhang S B, Wei S-H and Zunger A 1995 *Phys. Rev.* B **52** 13975
[44] Petit L, Schulthess T C, Svane A, Temmerman W M, Szotek Z and Janotti A 2006 *J. Electron. Mater.* **35** 556
[45] Qteish A 2000 *J. Phys.: Condens. Matter* **12** 5639
[46] Kobayashi M, Ishida Y, Hwang J I, Mizokawa T, Fujimori A, Mamiya K, Okamoto J, Takeda Y, Okane T, Saitoh Y, Muramatsu Y, Tanaka A, Saeki H, Tabata H and Kawai T 2005 *Phys. Rev.* B **72** 201201(R)
[47] Wi S C, Kang J-S, Kim J H, Lee S S, Cho S-B, Kim B J, Yoon S, Suh B J, Han S W, Kim K H, Kim B S, Song H J, Shin H J, Shim J H and Min B I 2004 *Phys. Status Solidi* b **241** 1529
[48] Tomiyasu K, Inami T and Ikeda N 2004 *Phys. Rev.* B **70** 184411
[49] Sato K, Katayama-Yoshida H and Dederichs P H 2005 *Japan. J. Appl. Phys.* **44** L948
[50] Katayama-Yoshida H, Sato K, Fukushima T, Toyoda M, Kizaki H, Dinh V A and Dederichs P H 2007 *Phys. Status Solidi* a **204** 15